Synthesis and application of functionally diverse 2,6,9-trisubstituted purine libraries as CDK inhibitors

Young-Tae Chang[1], Nathanael S Gray[1], Gustavo R Rosania[1], Daniel P Sutherlin[1], Soojin Kwon[1], Thea C Norman[1], Radhika Sarohia[1], Maryse Leost[2], Laurent Meijer[2] and Peter G Schultz[1]

Background: Purines constitute a structural class of protein ligands involved in mediating an astonishing array of metabolic processes and signal pathways in all living organisms. Synthesis of purine derivatives targeting specific purine-binding proteins *in vivo* could lead to versatile lead compounds for use as biological probes or drug candidates.

Results: We synthesized several libraries of 2,6,9-trisubstituted purines using both solution- and solid-phase chemistry, and screened the compounds for inhibition of cyclin-dependent kinase (CDK) activity and human leukemic cell growth. Lead compounds were optimized by iterative synthesis based on structure–activity relationships (SARs), as well as analysis of several CDK–inhibitor cocrystal structures, to afford several interesting compounds including one of the most potent CDK inhibitors known to date. Unexpectedly, some compounds with similar CDK inhibitory activity arrested cellular proliferation at distinctly different phases of the cell cycle, and another inhibitor directly induced apoptosis, bypassing cell-cycle arrest. Some of these compounds selectively inhibited growth of cells derived from specific tumors.

Conclusions: 2,6,9-Trisubstituted purines have various and potent biological activities, despite high concentrations of competing endogenous purine ligands in living cells. Purine libraries constitute a versatile source of small molecules that affect distinct biochemical pathways mediating different cellular functions.

Addresses: [1]Lawrence Berkeley National Laboratory and the Howard Hughes Medical Institute, Department of Chemistry, University of California, Berkeley, California 94720, USA, [2]C.N.R.S., Station Biologique, 29682 Roscoff, Bretagne, France.

Correspondence: Peter G Schultz
E-mail: pgschultz@lbl.gov

Key words: apoptosis, CDK inhibitor, cell-based assay, cell-cycle arrest, 2,6,9-trisubstituted purine library

Received: **3 February 1999**
Revisions requested: **1 March 1999**
Revisions received: **5 March 1999**
Accepted: **8 March 1999**

Published: **19 May 1999**

Chemistry & Biology June 1999, **6**:361–375
http://biomednet.com/elecref/1074552100600361

 ISSN 1074-5521

Introduction

Purines are ubiquitous molecules that exist at relatively high (millimolar) concentrations in living organisms. Guanine and adenine, two of the most common purines, are essential components of nucleic acids, cofactors and signaling molecules that modulate protein function. Indeed, more than 10% of the proteins encoded by the yeast genome evidently depend on a purine-containing ligand for their function (see the database search at http://www.quest7.proteome.com) [1]. These include kinases, DNA (or RNA) polymerases, ATPases, GTPases, purine receptors, and purine biosynthetic and metabolic enzymes. For this reason, diverse purine libraries might be expected to have a high probability of yielding bioactive compounds when screened in a variety of enzyme- and cell-based assays. It seemed likely that structural variation at the 2, 6, 8 and 9 positions might impart specificity towards a variety of target proteins. This possibility prompted us to explore purine libraries as a source of both drug leads and probes for analyzing complex cellular processes.

We chose first to screen our purine libraries for inhibitors of the cyclin-dependent kinases (CDKs) because CDKs have recently attracted considerable interest in light of their essential role in regulating the cell cycle. The CDKs are in turn regulated by a variety of intracellular signals including the binding of inhibitory factors, phosphorylation and cellular localization. Previously, a number of purines, as well as nonpurine compounds, such as olomoucine and staurosporine have been developed as CDK inhibitors, but they suffer from potency or selectivity problems, respectively (Figure 1). For example, purine analogs such as olomoucine and roscovitine have been shown to selectively inhibit a subset of the CDKs (olomoucine has an IC_{50} value of 7 μM against both CDK1 and CDK2 [2], and roscovitine has IC_{50} values of 0.65 and 0.7 μM against CDK1 and CDK2 [3]). A 2.4 Å resolution X-ray crystal structure of olomoucine bound to CDK2 revealed that the purine ring occupies the conserved ATP-binding pocket [4]. Unexpectedly, however, the purine ring of olomoucine is rotated nearly 180° with respect to that of ATP. Although the interactions between the amino-acid residues in the binding site are different for olomoucine and ATP, the amount of solvent-accessible surface that becomes buried is similar for the two ligands.

Figure 1

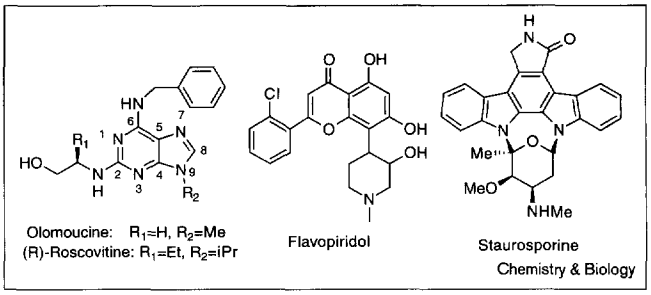

Structures of olomoucine, roscovitine, flavopiridol and staurosporine.

Although CDK1 and CDK2 serve different functions in controlling cell-cycle progression [5], the binding affinities of synthetic inhibitors [3] and the structures of their ATP-binding pockets are nearly identical, on the basis of amino-acid sequence [5]. Starting with the CDK2–olomoucine model, our goal is to use combinatorial chemistry to generate selective high-affinity inhibitors for CDK1 and CDK2, as well as other key cellular kinases, by introducing substituents at the 2, 6 and 9 positions of the purine ring. We and others previously reported several strategies for the solution- or solid-phase synthesis of purine derivatives [6–11], and have assayed these compounds against CDKs to determine structure–activity relationships (SARs). Our previous solid-phase synthesis scheme required that one position of the purine ring be held invariant to allow attachment to the solid support (Figure 2). Two positions were then varied combinatorially in order to identify optimal substituents in a pairwise fashion. In general, the effects of substituents at the 2, 6 and 9 positions on binding affinity appear to be additive, allowing one to rapidly identify potent purines by combining optimal substituents identified from simple binary libraries.

We describe new solid- and solution-phase syntheses of 2,6,9-trisubstituted purine libraries that can be used to combine rapidly and efficiently those substituents identified in the primary screens to afford second-generation libraries. Several specific and highly potent CDK2/CDK1 inhibitors have been identified from these libraries. In addition we characterized the cell-cycle inhibitory activities of a number of highly potent CDK inhibitors and found that some compounds arrested cellular proliferation at distinctly different phases of the cell cycle.

Results and discussion

Solid-phase synthesis

We used the crystal structures of various CDK2–ligand complexes to design the initial binary libraries with respect to the steric and electronic properties of the substituents to be introduced at the 2, 6 and 9 positions. A comparative analysis of the binding mode of olomoucine, flavopiridol [12] and staurosporine [13] in the ATP-binding pocket of CDK2 provided important information about functional groups that could be accommodated. For example, comparison of the bound purines and flavopiridol/staurosporine revealed that substituents at the 2 or 9 position of the purine ring might be able to occupy the same region of the active site as does the *N*-methyl piperidyl ring of flavopiridol (Figure 3c).

Synthesis and assays of the binary libraries against CDK2 indicated that aniline and 3- and 4-substituted benzylamine substituents led to significant improvements when introduced at the 6 position of the purine ring. Although a variety of hydroxyalkylamino, dihydroxyalkylamino and cycloalkylamino substituents at the 2 position resulted in moderate improvements, greater improvements were achieved with amino alcohols derived from valine and isoleucine. In contrast to many other protein kinases that can accommodate larger substituents at the 9 position of the purine ring, CDK2 binding was strongest for those purines bearing isopropyl functionality, followed by ethyl or hydroxyethyl [6].

Our previous synthetic routes involved tethering the purine core to the solid support through either a glycinamido, a 4-aminobenzyl amino or a 2-hydroxyethyl group at the 2, 6 and 9 positions, respectively. The drawback of these approaches is that one potential combinatorial site is lost. To circumvent this limitation a new solid-phase strategy and a versatile solution-phase route were developed. The solid-phase synthesis allows the introduction of substituents

Figure 2

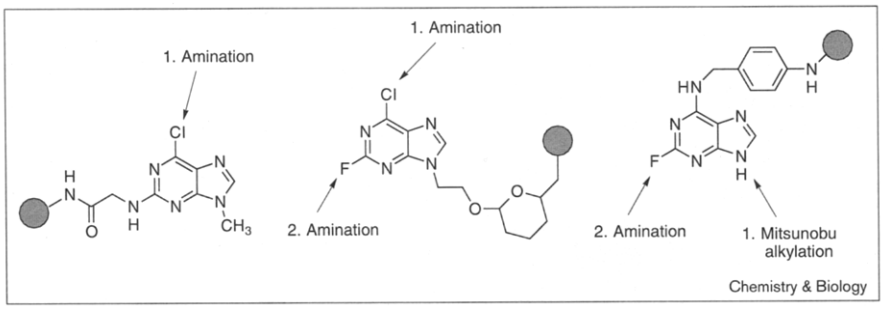

Precursors for binary library solid-phase synthesis.

Figure 3

Purvalanol B bound to CDK2 (black sticks, principal conformation only) is compared with **(a)** bound olomoucine (white sticks) and bound roscovitine (orange sticks), **(b)** bound ATP (yellow sticks), **(c)** bound flavopiridol (green sticks) and **(d)** bound staurosporine (purple sticks). The comparisons are based on superposition of the C_α atoms of CDK2. The ligands are shown in ball-and-stick representation with carbon atoms in white, nitrogen atoms in blue, oxygen atoms in red, phosphorous atoms in violet and the chlorine atoms of purvalanol B in green.

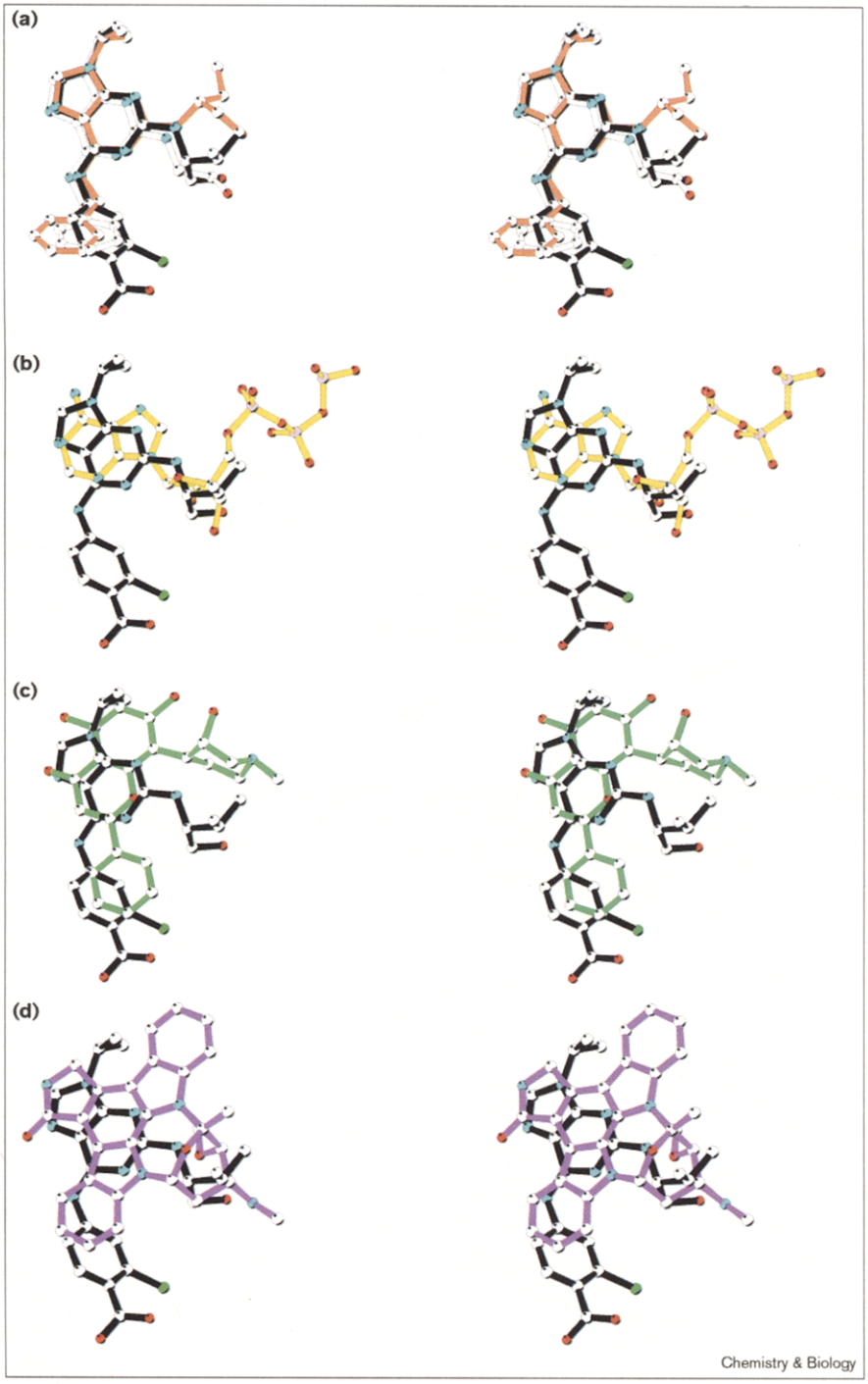

at the 2, 6 and 9 positions by immobilizing the purine through the N6 amino group. This is accomplished by starting with a library of resin-bound amines obtained from the reductive amination of a 5-(4-formyl-3,5-dimethoxyphenyloxy)valeric acid (BAL)-derivatized solid support with a collection of primary amines. By treating the resin-bound amines with a purine activated for substitution at the 6 position, combinatorial modification at the 6 position is achieved. Modification of the N9 and C2 positions is then accomplished using Mitsunobu and amination chemistry as described previously (Figure 4) [7].

The synthetic scheme outlined above required that the electrophilicity of the purine ring be increased so that the

Figure 4

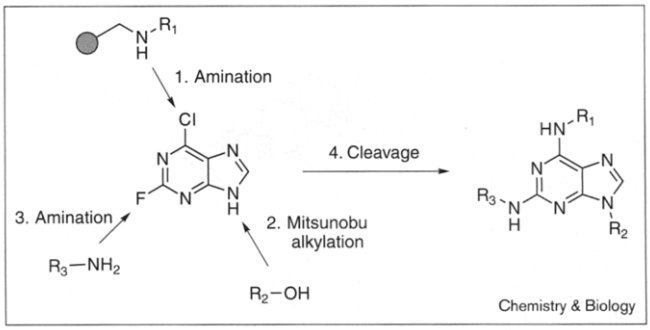

General scheme for solid-phase synthesis.

first amination reaction at the 6 position of the purine could be performed with weakly nucleophilic and α-branched amines. In order to facilitate the ability of a secondary amine to displace the 6-chloro group, we acylated the N9 position, which is expected to increase the overall electrophilicity of the purine ring. Unfortunately, the resulting activated amido group is more susceptible to nucleophilic attack than the 6-chloro group in the subsequent amination reaction. Another group that activates the 6 position of the purine ring without itself being susceptible to nucleophilic displacement is a N9-substituted tetrahydropyranyl (THP) aminal. Unfortunately, the acid lability of most commercially available solid supports made it difficult to cleave the THP group selectively without the concomitant release of the purine core. We therefore turned our attention to an N9-trimethylsilylethoxymethyl (SEM) activating group that is stable to amino nucleophiles and can be cleaved using fluoride under nonacidic conditions. The N9-SEM-2-fluoro-6-chloro purine **1** (Figure 5) was prepared (in 50% yield) by alkylation of 2-fluoro-6-chloropurine [7], with SEM-Cl in the presence of Hunig's base. This substitution significantly increased the reactivity of the ring system to amination, allowing an amination reaction with benzylamine to proceed at room temperature (which had previously required extended heating at 50°C).

The optimized scheme starts with the reductive amination of BAL-derivatized 4-methylbenzhydrylamine (MBHA) resin to give resin bound amine, **R2** [7]. A variety of amines including alkylamines, benzylamines and anilines were used in this first step. The purine core is then loaded onto solid support by reacting 2 equivalents of **1** with the amine-derivatized solid support **R2** at 50°C to give **R3**. The removal of the SEM protecting group was performed using 0.25 M tetrabutylammonium fluoride in THF at 60°C. The deprotected purine was then reacted with various alcohols and amines at the 9 and 2 positions using Mitsunobu and nucleophilic-substitution chemistry respectively, as is shown for 2-(3-hydroxypropylamino)-6-(4-methoxybenzylamino)-9-isopropylpurine (**209**; Figure 5).

Although we have used this solid-phase chemistry to prepare a variety of 2,6,9-trisubstituted purines, there are two limitations to this approach. First, secondary amines cannot be introduced at the 6 position because one nitrogen substituent is required to attach the amine to solid support. More significantly, amination at the 2 position with bulky groups proceeded in low yield, perhaps due to

Figure 5

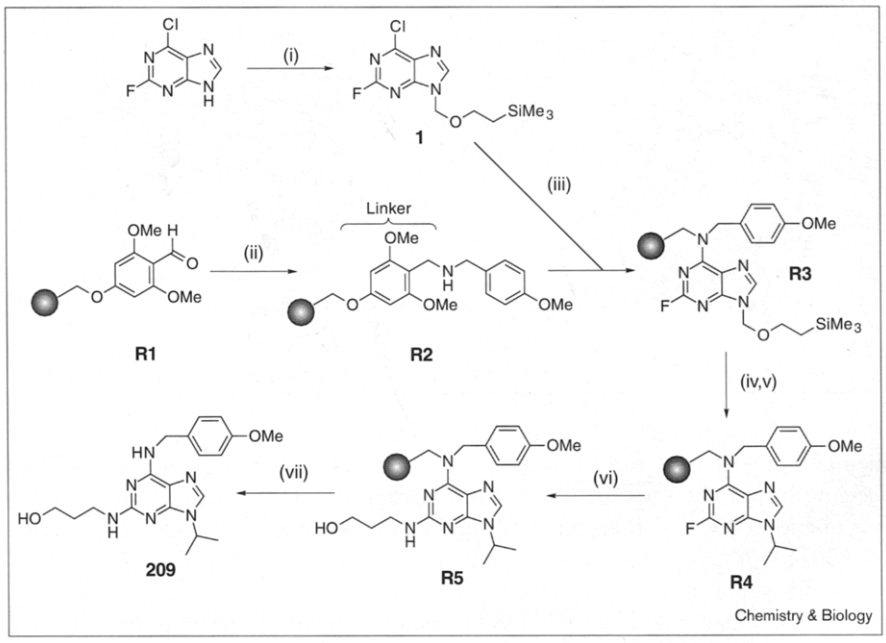

Representative scheme for solid-phase chemistry. **(i)** SEM-Cl (1.2 eq), DIEA, DMF, 0°C → rt. **(ii)** *p*-methoxybenzylamine, $NaBH(OAc)_3$, AcOH (2%), DMF, rt. **(iii)** DIEA, nBuOH-DMSO (1:1) 50°C. **(iv)** TBAF (0.25 M), THF, 60°C. **(v)** iPrOH (0.5 M), DIAD (0.5 M), PPh_3 (1.0 M), THF-CH_2Cl_2 (1:1). **(vi)** 3-amino-1-propanol, DIEA, *N*-methylpyrrolidinone, 110°C. **(vii)** TFA-water (95:5), rt.

Figure 6

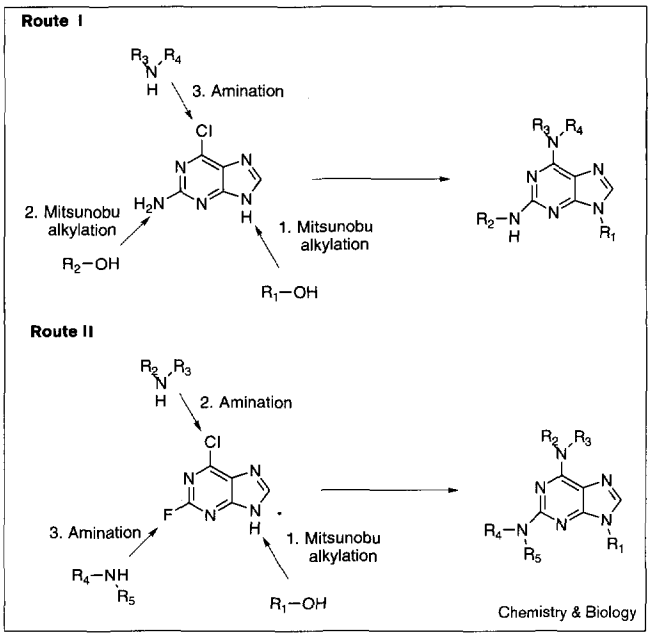

General schemes for solution-phase synthesis.

the decreased reactivity of purines attached to solid support. To overcome these limitations, we developed two versatile solution-phase synthetic routes to diverse trisubstituted purines.

Solution-phase synthesis

In route I (Figure 6), 2-amino-6-chloropurine was functionalized sequentially at the 9, 2 and 6 positions. Substituents at N9 were introduced by regioselective alkylation with a primary or secondary alcohol under Mitsunobu conditions [14]. In order to render the 2 position sufficiently acidic to undergo Mitsunobu alkylation, it was first acylated with trifluoroacetic anhydride. The trifluoroacetyl group is conveniently removed by hydrolysis with aqueous potassium carbonate prior to purification of the alkylated product by chromatography. Finally, a variety of primary and secondary benzylamines or anilines are introduced at the 6 position by reacting **3** with 1–2 equivalents of amine in *n*-butanol at elevated temperatures (Figure 7) (primary amines require 60°C whereas secondary amines and anilines require 110–120°C).

In route II (Figure 6), 2-fluoro-6-chloropurine was functionalized sequentially at the 9, 6 and 2 positions. As before, substituents at N9 position were introduced by Mitsunobu alkylation with either primary or secondary alcohols. This alkylation reaction tolerates virtually any alcohol without additional acidic hydrogens (pKa < 10–12). The more electrophilic 6-chloro substituent was selectively substituted with one equivalent of a benzylamine or aniline in analogy to route I. The resulting 2-fluoro-6,9-disubstituted purines were purified either by chromatography on silica or if solubility permitted, by trituration with dichloromethane and 0.1 N aqueous hydrochloric acid. Finally, the 2-fluoro position was aminated using an excess of primary or secondary amines in a small volume of *n*-butanol typically in a sealed tube (Figure 8). Representative procedures for two members of a purine library, **42** (synthesized by route I) and **60** (synthesized by route II), are shown in Figure 7 and 8.

CDK1/Cyclin B inhibition assay

Due to the limited information available concerning the N9 position SARs, we prepared a library to focus on this site. Libraries of 2-fluoro-6-(4-aminobenzylamino)-9-alkylpurines were synthesized using a 4-aminobenzylamino linkage strategy on resin-derivatized pins (Figure 2) [7]. In order to allow direct comparison of the efficacy of a range of substituents at the N9 position, a portion of the library was cleaved prior to amination at the 2 position. As can be seen from the assay results, optimal CDK2 inhibitory activity is observed for small alkyl groups with isopropyl exhibiting enhanced activity relative to ethyl, methyl and cyclopentyl (Figure 9). A similar result was obtained with another series of purines substituted with (*2R*)-pyrrolidin-2-yl-methanol at the C2 position [15].

To further enhance the CDK affinity of purine derivatives identified in previous screens of first-generation purine libraries, the synthetic methods described above were iteratively applied to the 2, 6 and 9 positions, and compounds were tested for activity against starfish oocyte CDK1/cyclin B [3]. Based on the improved activities of a 9 position isopropyl over methyl, and aniline over the benzyl group of olomoucine, we first derivatized the 9 position with an isopropyl substituent and tested various aniline substituents at the 6 position (Figure 10). Among the 2,3,4-substituted anilines, the 3-chloroaniline derivative **52** is the best CDK

Figure 7

Representative scheme I for solution chemistry. **(i)** iPrOH (2.0 eq), DEAD (1.1 eq), PPh_3 (2.0 eq),THF, −10 → 25°C. **(ii)** $(CF_3CO)_2O$, CH_2Cl_2, 0 → 25°C. **(iii)** $TBDMSOCH_2CH_2OH$ (2.0 eq), DEAD (1.0 eq), PPh_3 (2.0 eq), THF, 0 → 25°C. Then K_2CO_3, MeOH. **(iv)** aniline (4.0 eq), DIEA, nBuOH, 110°C. Then AcOH-H_2O-THF (3:1:1).

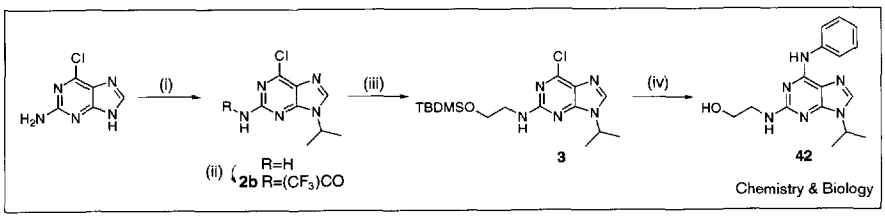

Figure 8

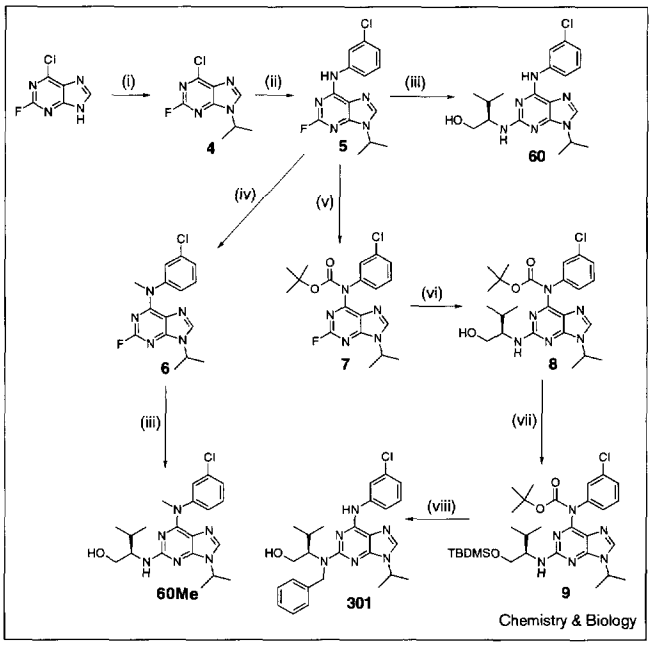

Representative scheme for solution chemistry II. **(i)** iPrOH (1.2 eq), DEAD (1.3 eq). PPh_3 (1.3 eq), THF −10 → 25°C. **(ii)** 3-chloroaniline (1.0 eq), DIEA, nBuOH, 140°C. **(iii)** (*R*)-(−)-2-amino-3-methyl-1-butanol (1.5 eq), DIEA, nBuOH, 150–170°C in sealed tube. **(iv)** MeI (2 eq), NaH, DMF, rt. **(v)** Boc_2O, DIEA, DMAP, THF, rt. **(vi)** (*R*)-(−)-2-amino-3-methyl-1-butanol (1.2 eq), DIEA, DMSO, 70–80°C. **(vii)** TBDMS-Cl, imidazole, DMAP, THF, rt. **(viii)** BnBr, Bu_4NI, NaH, DMF. Then pTSA, MeOH-CH_2Cl_2, rt.

inhibitor, showing a 30-fold improvement over olomoucine (with an IC_{50} value of 220 nM). The 3-bromo, fluoro and trifluoromethyl groups exhibited comparable activities, whereas the same 2-substituted purines are tenfold less active.

Next, we explored variations at the 2 position with the 6 position derivatized with either 4-methoxybenzylamine, the best among the benzyl substituents or 3-chloroaniline, chosen from the first-round solution-phase synthesis (Figure 11). Many compounds that have moderate activity (100–1000 nM) were found in this series. In general, we observed a preference for hydroxyalkyl or dihydroxyalkyl groups at the 2 position. An eightfold improvement in the IC_{50} value, however, was obtained by replacing the 2 position hydroxyethylamino (**52**) with *R*-valinol attached via the α-amino group (**60**, named purvalanol A). In agreement with other reports [3], compounds with the *R*-stereochemistry were 2–16-fold more potent than those with the *S*-stereochemistry (**75** versus **76**, **60** versus **58**, **66** versus **59** and **68** versus **69**). Although most of the cyclic secondary amines were in general not preferred at 2 position, 2-hydroxyethylpiperidyl (**10**) improved the inhibitory activity threefold over hydroxyethyl (**118**).

In the third round, we fixed the 2 position with the *R*-valinol substituent, and refocused attention to the 6 position with a variety of benzylamine and aniline groups (Figure 12). This resulted in a set of the most active small-molecule CDK inhibitors known to date. The halogens on the 3 and 4 positions significantly improved the activity, and both the activity and solubility were enhanced with an additional carboxylate or amino group.

In parallel with the third round, we also fixed the 2 position with 2-(2-hydroxyethyl)piperidyl substituent and derivatized the 6 position with various benzylamine and aniline substituents (Figure 13). Simple aniline (**220**) or

Figure 9

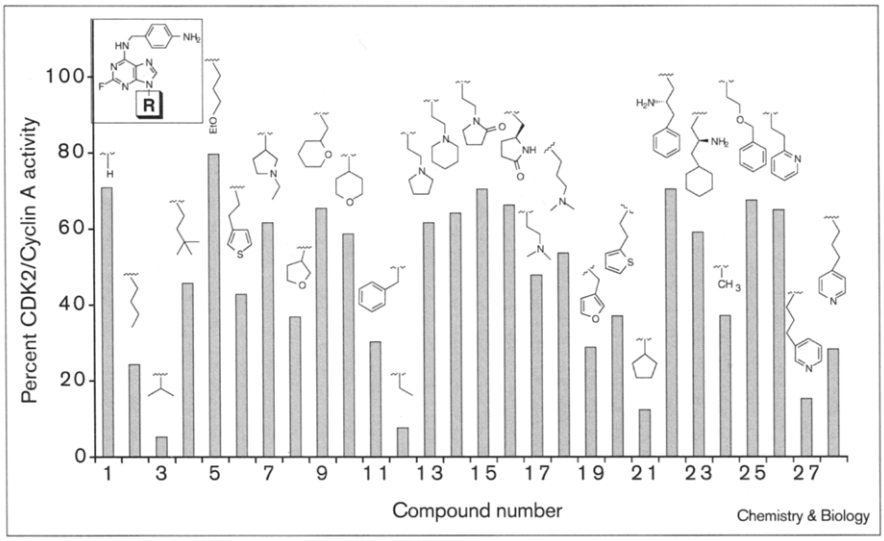

CDK2/cyclin A activity for representative compounds from an N9-directed library.

Figure 10

SAR class 1. Various C6-substituents on a 2-(2-hydroxyethylamino)-9-isopropylpurine core.

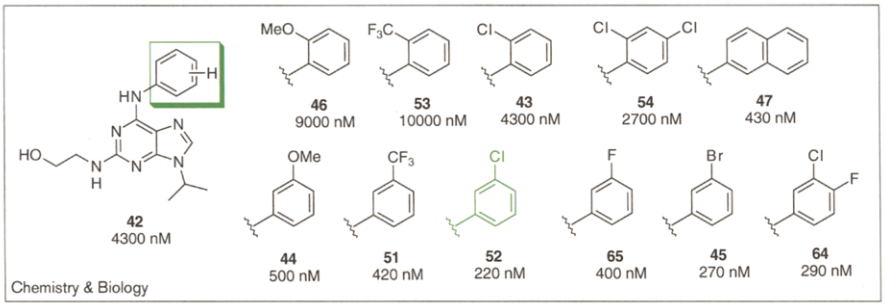

benzylamine (**212**) substituents proved to be slightly better than 4-methoxybenzylamine (**10**). Although 4-substituted benzylamine was tolerated (**216**), 3-substituted benzylamine (**113**, **222**) decreased the activity significantly. Linear alkyl substituents (**219**), bulky substituents (**225**, **226**, **227**) and substituted anilines (**359**, **306**) also decreased the activity.

During these rounds of optimization, we relied on the approximate additivity of substituents. The observed additivity allowed us to more efficiently assess greater numbers of substituents at a single site, thereby enhancing our ability to explore each of the binding sites without having to make all combinatorial possibilities. In this format, evaluation of 10 substituents at each site requires three sets of 10 compounds rather than one set of 1000. The simplest explanation for the observed additivity is that the rigid purine scaffold prevents substituents at the 2, 6 and 9 positions from binding in overlapping regions of the active site.

One of our most potent inhibitors, purvalanol B (**95**; Figure 12), was cocrystalized with CDK2 (Figure 14) [16], and the structure was compared with the structures of CDK2–flavopiridol, CDK2–staurosporine and CDK2–ATP (Figure 3). Purvalanol B occupied 86% of the available space in the binding pocket of CDK2, whereas flavopiridol occupied 74%, ATP occupied 78% and olomoucine occupied 76%.

Another of the most potent inhibitors, aminopurvalanol (**97**; Figure 12) was tested for its activity against a variety of kinases (Table 1). As expected, aminopurvalanol had almost the same activity against CDK1 as CDK2, with IC_{50} values ranging from 28–33 nM. Among the enzymes tested, only CDK5/p35 was inhibited to the same extent as CDK1/CDK2, whereas other kinases exhibited much weaker inhibition by **97**. The high degree of specificity observed for **97** is similar to that observed for purvalanol A and B [16].

The crystal structures of CDK2 with purvalanol B, ATP, flavopiridol or staurosporine suggested that additional contacts could be introduced by appending an extra group at the N2 position of purvalanol B (Figure 14). We therefore attempted to synthesize N2-disubstituted derivatives of **60** by amination of 2-fluoro-6-(3-chloroanilino)-9-isopropylpurine (**5**) with *N*-alkyl valinol derivatives. Several *N*-alkyl valinol derivatives were synthesized by reductive alkylation of valinol with a variety of alkyl, aromatic and heteroaromatic aldehydes using sodium triacetoxyborohydride in 1,2-dichloroethane. Unfortunately, these branched secondary amines could not be installed at the 2 position, presumably due to their steric bulkiness. Attempts to activate the 2-fluoro group by introducing an electron withdrawing *tert*-butoxycarbonyl (Boc) group at the 6-position also failed to promote nucleophilic substitution. Finally, the O-silyl and 6-N-Boc protected derivative, **9**, was successfully alkylated using sodium hydride, alkyl halide and tetrabutylammonium iodide in dimethylformamide (Figure 8). The desired compounds were obtained by removing the protecting groups and tested against CDK1/cyclin B. Unexpectedly, this class of compounds showed substantially reduced activity (with an IC_{50} value between 5 and 10 μM; Figure 15). This is not simply a consequence of disubstitution at the 2 position because 2-bishydroxyethyl derivatives such as **16**, **26**, **211**, **303**, **304** and **305** (IC_{50} 220–350 nM) show comparable activity to their parent hydroxyethyl derivatives **118** (IC_{50} 700 nM), and **52** (IC_{50} 220 nM; Figure 11). Potentially the combination of the sterically hindered *R*-valinol with additional substitution at the 2 position may prevent the inhibitors from accessing a productive binding conformation. Alternatively, the hydrophobic *N*-alkyl valinol derivatives that we introduced at the 2 position might have been poorly suited to the binding site.

For many of the biological applications described in the next section, we wanted access to a collection of negative control compounds that were structurally very similar to our potent inhibitors but lacked CDK inhibitory activity. We could then use these inactive derivatives to test if an observed *in vivo* effect is correlated with *in vitro* CDK activity. From the cocrystal structure of purvalanol B with CDK2 it was apparent that addition of a methyl group to N6 should lead to significantly reduced CDK inhibitory activity due to steric hindrance and the loss of a hydrogen

Figure 11

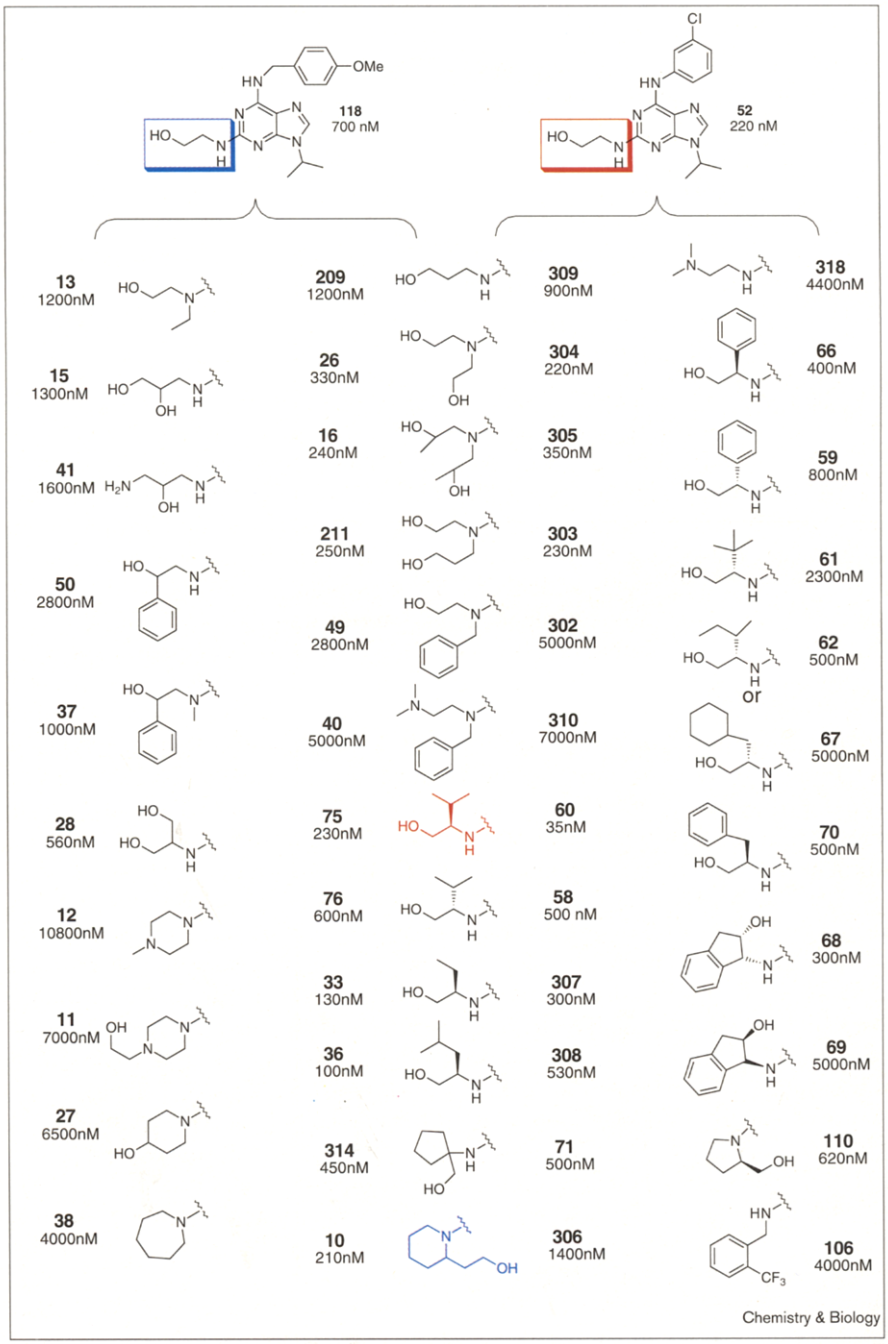

SAR class 2. Various C2-substituents on a 6-(4-methoxybenzylamino)- or a 6-(3-chloroanilino)-9-isopropylpurine core.

bond to Leu83 (Figure 14). We synthesized N6-methylated derivatives of four of our most potent CDK inhibitors (**52**, **60**, **97** and **212**; Figure 8). As expected, these compounds (**52Me**, **60Me**, **97Me** and **212Me**) are completely inactive as CDK1/cyclin B inhibitors *in vitro*.

Cellular effects and cell cycle studies

We investigated the biological activity of the most potent CDK inhibitors from each SAR class by testing their ability to inhibit growth of U937 human leukemic cells. Cell populations were treated with the various compounds, and then assayed for the percentage decrease in the number of viable cells, using the 3-(4,5-dimethylthiazole-2-yl)-2,5-diphenyl-2H-tetrazolium bromide (MTT) assay [17]. The most potent CDK inhibitors in SAR classes 2 and 3 (Figures 11 and 12), compounds **60** and **97**, were also found to be active inhibitors of cell growth (with IC_{50} values of 7.5 and 5 μM, respectively). The significant increase in the

Figure 12

SAR class 3. Various C6-substituents on a 2-(1*R*-isopropyl-2-hydroxyethylamino)-9-isopropylpurine core.

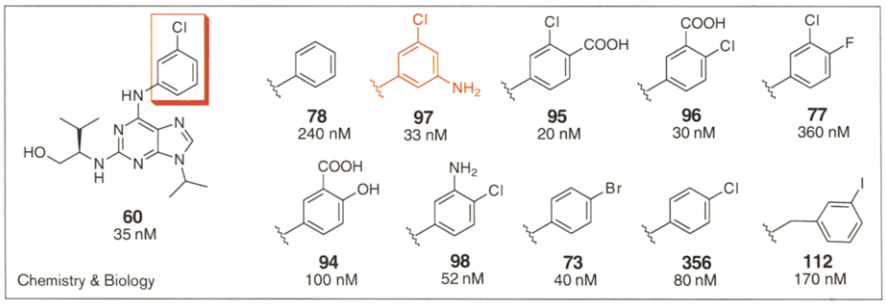

cell-based IC_{50} values relative to the *in vitro* IC_{50} values is presumably a result of competition with high concentrations of intracellular ATP (estimated to be in the millimolar range). Indeed when the kinase assay concentration of ATP was increased from 15 μM to 1.5 mM, the IC_{50} value for compound **60** increased (as expected) from 4 nM to 500 nM [16]. Compounds **94** and **95** were equally active in the kinase assay but inactive *in vivo*, probably due to the decreased cell permeability resulting from the negatively charged carboxylate group. From SAR class 4 (Figure 13), **212** is both a potent inhibitor of CDK activity and of cell growth (IC_{50} = 2.5 μM).

To study the specific effects of different purine derivatives on cell-cycle progression, unsynchronized proliferating U937 cells were treated with compounds **60**, **97**, **212** and **52**. Treated cells were then subjected to cell-cycle analysis using flow cytometry and to morphological analysis using fluorescence microscopy. For flow cytometry, unsynchronized cell populations were labeled with propidium iodide (PI), a fluorescent DNA intercalator, and for the TUNEL assay, with a marker of DNA fragmentation that is characteristic of apoptosis. For morphological analysis, cells were labeled with Hoescht 33258, a DNA-specific dye, and with an antitubulin antibody that could be visualized using a FITC-conjugated secondary antibody. Using dose-response and time-course assays, differences in the effects of the compounds due to variations in compound permeability or the kinetics of the cellular response were investigated.

Initially, U937 cell populations were examined after treatment with **97** or **60**, the most potent and bioactive CDK inhibitors. By flow cytometry, treatment of cells with **97** or **60** at doses lower than 10 μM specifically arrested cells in the G2–M phase of the cell cycle, based on the accumulation of cells with a 4 N DNA content, and the absence of DNA fragmentation (Figure 16). At higher concentrations (≥ 20 μM), however, both **97** and **60** triggered apoptosis after 8 h treatments, as detected with the TUNEL assay and confirmed by the appearance of nucleosome-sized DNA ladders as assessed by electophoresis (data not shown). The only apparent difference between the effects conferred by **60** or **97** to proliferating U937 cells related to their specific activity: **97** was four times more active than **60** in inducing a G2–M cell-cycle arrest (with IC_{50} values of 1.25 μM and 5 μM, respectively). The effect of **97** and **60** on microtubule architecture and on chromatin condensation were consistent with G2 cell-cycle arrest, based on the low percentage of mitotic cells (< 5%) seen in the treated populations. Because entry into mitosis depends on CDK1/CDK2 activity [18], inhibition of the G2–M phase transition was the expected result, based on the high activity of the compounds against CDK *in vitro*. Indeed, cells treated with either compound displayed fibrous microtubule organization, decondensed chromatin and intact nuclear architecture characteristic of interphase cells. Nevertheless, consistent with centrosome duplication occurring independently of CDK1 activity [19], a significant fraction of cells possessed two distinct

Figure 13

SAR class 4. Various C6-substituents on a 2-(2-hydroxyethylpiperidyl)-9-isopropylpurine core.

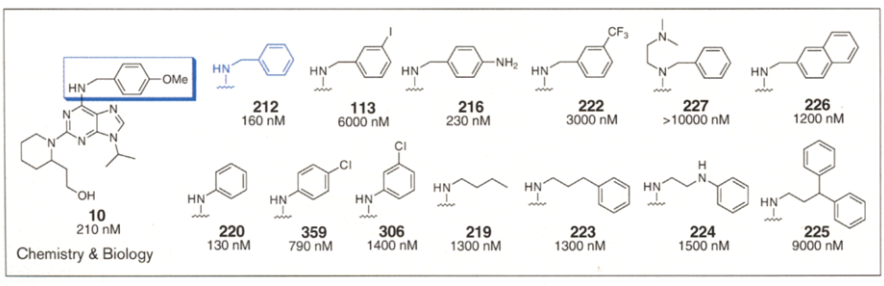

Figure 14

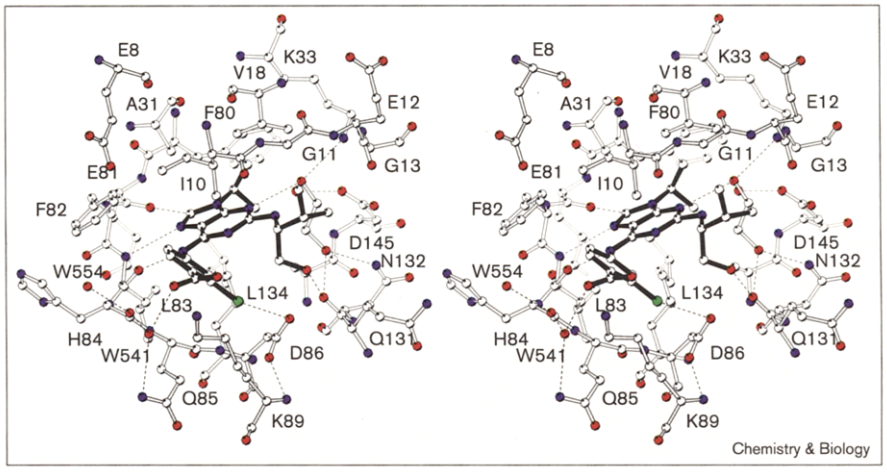

Binding site structure of CDK2–**95** (purvalanol B).

microtubule arrays nucleated by discernible microtubule-organizing centers (Figure 17). In the presence of **97**, these duplicated microtubule-organizing centers nucleated long microtubules characteristic of interphase cells. In the presence of **60**, some of the microtubule arrays appeared shorter and more polarized, reminiscent of half spindles without attached chromosomes. Based on these results, the effects of compounds **60** and **97** on proliferating U937 cells appeared consistent with their specific CDK1/CDK2 inhibitory activity.

The CDK inhibitory activity of compounds **60** and **97** was significantly different from that of **52**, the most potent CDK1 inhibitor from SAR class 1 (Figure 10). By flow cytometry, **52** affected cell-cycle progression at concentrations of 25 μM or greater. Unlike cells treated with **60** or **97**, however, cells treated with a comparable concentration of **52** did not become apoptotic (Figure 16b) and did not exhibit the characteristic accumulation of cells with a 4 N DNA content indicative of a G2 arrest. Instead, **52**-treated cell populations displayed a reproducible depletion of the late-S/early-G2 cell population (Figure 16a). Morphologically, more than 20% of the cell population treated with **52** had bipolar microtubule spindles and condensed chromosomes, compared with less than 5% in control cell populations. This indicates that treatment of U937 cells with **52** causes arrest at mitosis. Interestingly, all of the **52**-arrested, mitotic cells were in metaphase, as judged by the presence of two centrosomes, which nucleated polarized microtubules that were oriented towards each other, and fully condensed chromosomes aligned at the equator. Given the structural

Table 1

Inhibition of purified kinases by aminopurvalanol (97).

Kinase	IC_{50} (μM)
CDK1/cyclin B	0.033
CDK2/cyclin A	0.033
CDK2/cyclin E	0.028
CDK5/p35	0.020
Erk1	12.0
Erk2	3.1
c-Raf	>100
MAPKK	>100
PKC-α	>100
PKC-β1	>100
PKC-β2	>100
PKC-γ	>100
PKC-δ	36.0
PKC-ε	>100
PKC-η	>100
PKC-ζ	>100
PKA	18.0
PKG	>100
Casein kinase 1	3.0
Casein kinase 2	>100
Insulin receptor Tyr-K	4.4

Figure 15

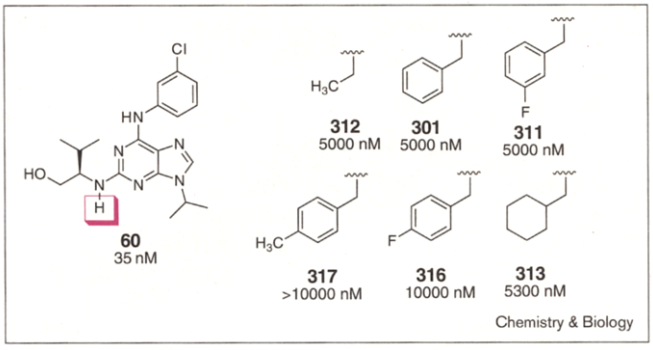

SAR class 5. Various C2-substituents on a 2-((1*R*-isopropyl)-2-hydroxyethylamino)-6-(3-chloroanilino)-9-isopropylpurine core.

Figure 16

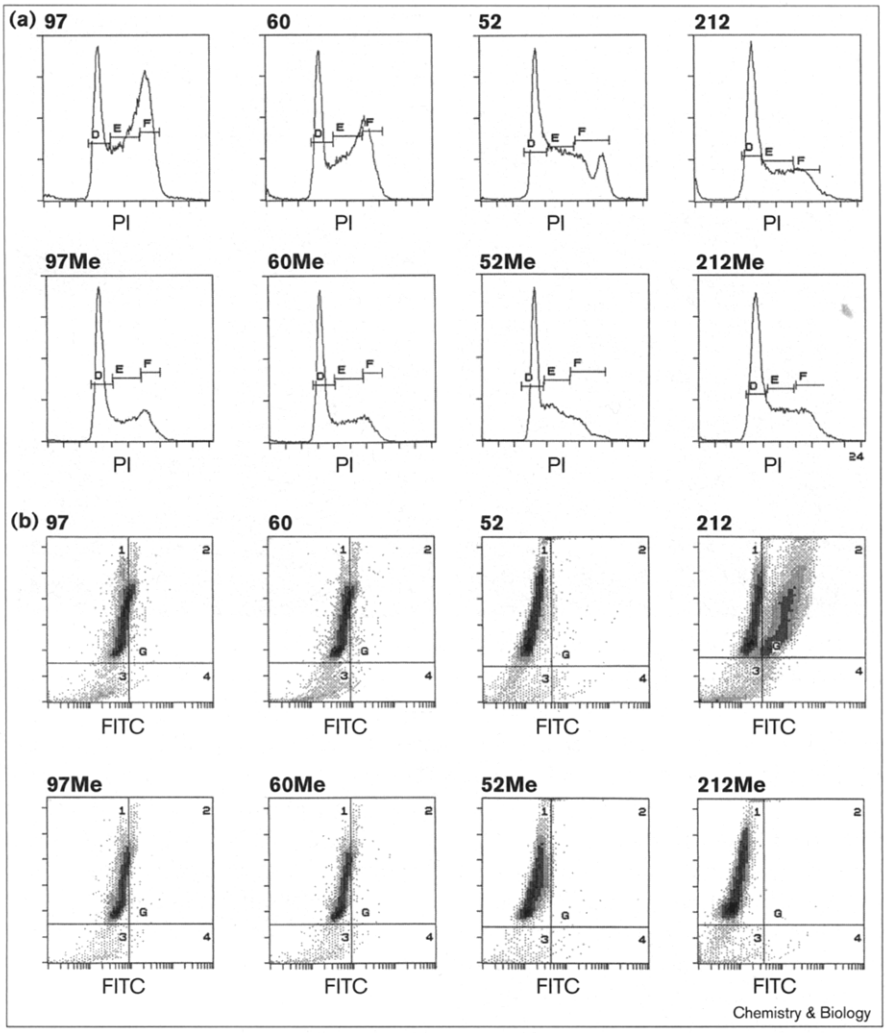

Flow cytometric analysis of **(a)** cell-cycle distribution and **(b)** apoptosis in U937 cell populations treated with different CDK inhibitors and their inactive, N6-methylated analogs. For each experiment, cells were treated for 0, 2, 4, 6 or 8 h, with increasing concentrations of compounds. Plots represent the most specific effect of each compound, as determined with the dose-response and time-course assays. For all the experiments, cells were co-labeled with PI, to stain the DNA, and with the TUNEL assay, to incorporate FITC-labeled nucleotides onto the ends of DNA fragments resulting from the apoptotic process. (a) Plots showing the distribution of cells with different DNA contents, after 8 h treatment with 5 μM **97** or **97Me**, 10 μM **60** or **60Me**, 50 μM **52** or **52Me** or 5 μM **212** or **212Me**. Bars indicate approximate DNA contents of cells with a 2N (D), intermediate (E) and 4N (F) DNA content, characteristic of cells in G1, S or G2-M phases of the cell cycle, respectively. DNA distribution of untreated cell populations are similar to those treated with the inactive, N6-methylated derivatives. (b) Bivariate plots of FITC versus PI staining of the same cell populations as in (a). Note that **212** is the only compound that nonspecifically induces apoptosis throughout the cell cycle without changing the cell-cycle distribution of the treated cell population.

similarity between compounds **52** and **60**, we were surprised by their different effects on cells.

The effect of **212**, one of the most potent CDK inhibitors from SAR class 4 (Figure 13), on proliferating U937 cell populations was also different from that of **52**, **60** or **97**. Flow cytometric analysis revealed that compound **212** was a nonspecific inducer of apoptosis at concentrations as low as 5 μM: it triggered DNA fragmentation at all phases of the cell cycle, without affecting cell-cycle progression (Figure 16). With the TUNEL assay, the effects of **212** could be observed at concentrations as low as 2.5 μM, making this compound one of the most potent inducers of apoptosis in the library. The induction of apoptosis was confirmed by the electrophoretic demonstration of nucleosome-sized DNA from the **212**-treated cells (data not shown). Morphologically, cells treated with **212** exhibited characteristic apoptotic features, such as condensed DNA, fragmented nuclei and little microtubule staining (Figure 17). By phase-contrast microscopy, cellular fragmentation was also apparent (data not shown).

As controls, the N6-methylated derivatives of **52**, **60**, **97** and **212** were tested side-by-side with the respective active non-methylated compounds. At the same concentrations as the active analogs, none of the control compounds induced the cell-cycle effects, apoptosis, nor the abnormal microtubule features (Figures 16,17). It appears, therefore, that although closely related purine derivatives had different effects when tested on cultured cells, the effects of the compounds on cell-cycle progression were specifically related to their chemical structure and their CDK-inhibitory activity. Previously, treatment of cells with olomoucine or roscovitine had been reported to lead to a G1/S and G2/M cell cycle arrest by a single mechanism [12,20,21]. In contrast, the different effects of these more potent and specific CDK inhibitors indicates a broader spectrum of activity. It remains to be determined whether the selectivity of different purines is

Figure 17

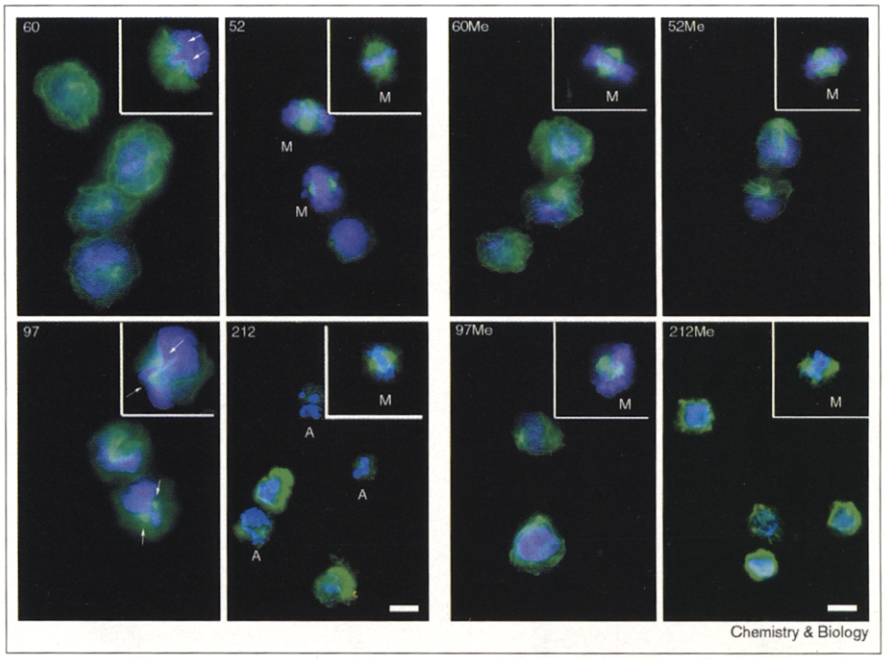

Morphological analysis of U937 cells treated with different CDK inhibitors and their inactive, N6-methylated analogs. For these experiments, cells were treated with the selected compounds for 6 h. Cells were then stained with fluorescein antitubulin immunocytochemistry to label the microtubules (green) and with the DNA-specific dye Hoescht 33258 to label the chromatin (blue). Samples were analyzed under the fluorescence microscope. Insets show the representative morphology of cells possessing duplicated microtubule organizing centers. In **60** and **97**, arrows indicate the abnormal, interphase-like microtubule arrays nucleated from these duplicated microtubule organizing centers. Note that the chromatin remains decondensed in these cells. Unlabeled cells are those with interphasic microtubule arrays and decondensed chromatin. M, cells with mitiotic bipolar spindles and condensed chromosomes. A, cells with apoptotic features such as condensed or fragmented nuclei accompanied by little microtubule staining.

related to the specific molecular mechanism of cell-cycle deregulation accompanying cellular transformation.

Cell-type selectivity study

Because different tumors are characterized by genetic defects affecting different cell-cycle regulatory pathways, it has been hypothesized that compounds that act upon a specific pathway might be able to selectively inhibit growth of a particular tumor. Given the multiplicity of cell-cycle inhibitory activities exhibited by the purine inhibitors described, it seemed plausible that different purines would show selective growth-inhibitory activity against different tumor cell lines. Several active purines (**60**, **75**, **95**, **97** and **212**) were therefore selected for testing against the National Cancer Institute (NCI) panel of 60 cancer cell lines derived from different tumors. Cell growth inhibitory and cytotoxic activities of the compounds were found in the micromolar to nanomolar range. Although **75** and **212** were less selective to different cell types, **60** and **97** showed significant selectivity to KM12 colon cancer cells (Table 2). Compound **95** did not show significant cytotoxicity in these cell lines, presumably due to its decreased cell permeability.

Table 2

GI_{50} values for selected cancer cell lines (μM).

	52	**60**	**75**	**97**	**212**
IGROV1 (ovarian cancer)	6.9	0.98	5.0	0.47	0.79
SR (leukemia)	7.6	1.9	2.3	0.42	4.7
NCI-H522 (lung cancer)	2.6	0.35	1.9	1.0	1.4
KM12 (colon cancer)	7.4	0.076	1.4	0.030	1.2
Average GI_{50}*	14	2.0	3.7	1.8	2.1
Average TGI†	53	10	17	8.1	9.8
Average LC_{50}‡	91	66	65	35	35

*GI_{50}, growth inhibitory effect. †TGI, cytostatic effect. ‡LC_{50}, cytotoxic effect.

Significance

Purine ligands are bound by a tremendous variety of enzymes in living organisms. Synthetic purine derivatives with diverse substituents may have the ability to bind selectively to one class of purine-recognizing enzymes. We synthesized several hundred 2,6,9-trisubstituted purine derivatives using solid- and solution-phase chemistry and screened them for inhibition of cyclin-dependent kinase (CDK1)/cyclin B. In addition to finding several highly specific and potent CDK inhibitors, we identified several compounds that elicited significantly different effects when tested in living cells. Compounds 60 (purvalanol A) and 97 (aminopurvalanol) arrest the cell cycle specifically in the G2 phase and induced morphological features consistent with their observed CDK1/CDK2 inhibitory activity. In contrast, compound 52, a moderate CDK inhibitor, induced M-phase arrest, and compound 212, also an active CDK inhibitor, induced apoptosis independent of cell-cycle phase. This broad spectrum of biological activities suggests that different purines might selectively act on different biochemical pathways affecting cell-cycle progression.

The degree of specificity exhibited by some of these purines, in terms of their ability to inhibit the cell-division cycle at different stages, is quite remarkable. Indeed, both structure–activity relationship (SAR) studies and the complete inactivity of the *N*-methylated analogs indicate that the effects of the different compounds are closely related to their chemical structures and to their CDK inhibitory activity. One possible interpretation of how similar CDK inhibitors display different cell-cycle inhibitory activities is that they are inhibiting different kinases *in vivo*. Alternatively, they might be inhibiting different activities of the same CDK, complexed with specific cyclins conferring different substrate specificities.

Materials and methods

Representative solution phase synthesis

2-Amino-6-chloro-9-isopropylpurine ***(2a)***. Anhydrous THF (120 ml) was added to a flame-dried flask under nitrogen containing 2-amino-6-chloropurine (2.0 g, 11.8 mmol) and triphenylphosphine (6.2 g, 23.6 mmol). To this was added 2-propanol (1.4 ml, 23.6 mmol), after which the solution was stirred and cooled to −10°C using an ethyleneglycol/dry-ice bath. Following the dropwise addition of diethyl azodicarboxylate (2.0 ml, 13.0 mmol), the mixture was gradually warmed to rt. After 24 h, the reaction was quenched with 2-propanol (1.5 ml) and the solvent was removed *in vacuo*. The resulting yellow/white gum was purified by column chromatography (1000 ml SiO_2, eluted sequentially with 99:1 and then 98:2 CH_2Cl_2:MeOH) to afford 2.9 g of **2a** as a colorless foam (this product was contaminated with triphenylphosphine oxide and the diethyl hydrazine-N,N′-dicarboxylate ester byproducts). The crude product was trifluoroacetylated without further purification. An analytical sample was prepared using preparative thin-layer chromatography (TLC; 1.0 mm thickness, developed with 95:5 CH_2Cl_2:MeOH). Rf 0.35 (CH_2Cl_2:MeOH 95:5); ^{1}H NMR (400 MHz, $CDCl_3$) δ 1.58 (d, 6H, 6.8 Hz), 4.70 (sept., 1H, 6.8 Hz), 5.29 (br s, 2H), 7.85 (s, 1H); ^{13}C NMR (101 MHz, $CDCl_3$) δ 22.3, 47.1, 125.6, 140.0, 151.1, 153.4, 158.8; mass spectrum (FAB$^+$) m/e 212 (MH^+); HRMS calc'd for $(C_8H_{10}N_5Cl)H^+$: 212.0703, found: 212.0703.

2-Trifluoroacetamino-6-chloro-9-isopropylpurine ***(2b)***. 2-Amino-6-chloro-9-isopropylpurine (3.11 g, 14.7 mmol) was dissolved in distilled CH_2Cl_2 (29 ml) and the resulting solution cooled to 0°C. Trifluoroacetic anhydride (6.2 ml, 44 mmol) was added dropwise. The reaction mixture was warmed to rt over 3 h, concentrated *in vacuo* and dried further under high vacuum. The crude product was purified by chromatography (600 ml SiO_2, eluted with 20:80 EtOAc:CH_2Cl_2) to yield 4.0 g of **2b** (88%). Rf 0.41 (CH_2Cl_2:MeOH 95:5); ^{1}H NMR (400 MHz, $CDCl_3$) δ 1.68 (d, 6H, 6.8 Hz), 4.92 (sept., 1H, 6.8 Hz), 8.59 (s, 1H), 10.20 (s, 1H).

2-(2-tert-Butyldimethylsilyloxyethylamino)-6-chloro-9-isopropylpurine ***(3)***. Trifluoroacetamide **2b** (4.52 g, 14.7 mmol), 2-*tert*-butyldimethylsilyloxyethanol (5.18 g, 29.4 mmol) and triphenylphosphine (7.71 g, 29.4 mmol) were dissolved in freshly distilled THF (500 ml). The reaction mixture was stirred and cooled to 0°C and diethyl azodicarboxylate (2.31 ml, 14.7 mmol) was added dropwise over 5 min. The reaction mixture was warmed to rt, stirred for 12 h, and concentrated *in vacuo* to yield a yellow oil. This crude reaction mixture was redissolved in methanol (50 ml) and combined with an aqueous solution of potassium carbonate (16 ml, 1.0 M). The hydrolysis was complete within 1 h as judged by the disappearance of the trifluoroacetamide (Rf 0.74 EtOAc:hexane 75:25) by TLC. The resulting white slurry was partitioned between ethyl acetate and water (300 ml of each) and the organic layer collected, dried over sodium sulfate and concentrated *in vacuo*. The resulting oil was purified by column chromatography (1000 ml SiO_2, eluted with EtOAc:CH_2Cl_2 5:95) to yield 3.0 g of **3** (55%). Rf 0.26 (EtOAc:hexane 1:1); ^{1}H NMR (500 MHz, $CDCl_3$) δ 0.06 (s, 6H), 0.90 (s, 9H), 1.57 (d, 6H, 6.8 Hz), 3.57 (q, 2H, 5.6 Hz), 3.80 (t, 2H, 5.6 Hz), 4.69 (sept., 1H, 6.8 Hz), 5.49 (bs, 1H), 7.76 (s, 1H); ^{13}C NMR (126 MHz, $CDCl_3$) δ −4.8, 21.1, 24.8, 25.0, 43.5, 47.2, 60.2, 123.1, 139.7, 149.8, 152.7, 158.5; mass spectrum for $C_{16}H_{28}N_5ClOSi$ (FAB$^+$) m/e 371 (MH^+).

2-(2-Hydroxyethylamino)-6-anilino-9-isopropylpurine ***(42)***. Compound **3** (24 mg, 0.06 mmol), aniline (24 µl, 0.26 mmol) and diisopropylethylamine (45 µl, 0.26 mmol) were dissolved in *n*BuOH (1.5 ml). The reaction mixture was stirred at 90°C for 12 h and then concentrated *in vacuo*. The crude product was dissolved in a mixture of THF (200 µl), water (200 µl) and acetic acid (600 µl). The reaction mixture was stirred at rt for 12 h, concentrated *in vacuo* and azeotroped 3 × with methanol (3 ml × 3). The crude product was purified by preparative TLC (2 plates 1.0 mm thickness, developed twice with 60:40 EtOAc:hexane) to yield 16.4 mg (81%) of 42 as an oil. ^{1}H NMR (400 MHz, $CDCl_3$): δ 1.52 (d, 6H, 6.8 Hz), 3.59–3.63 (m, 2H), 3.84–3.87 (m, 2H), 4.57–4.65 (m, 1H), 5.51–5.53 (m, 1H), 7.03–7.07 (m, 1H), 7.27–7.33 (m, 2H), 7.59 (s, 1H), 7.75–7.77 (m, 2H), 8.16 (s, 1H); ^{13}C NMR (126 MHz, $CDCl_3$) δ 22.4, 45.1, 46.6, 63.8, 114.8, 120.2, 123.0, 128.7, 135.0, 139.1, 150.5, 152.4, 160.6; mass spectrum (FAB$^+$) m/e 313 (MH^+); HRMS calc'd for $(C_{16}H_{20}N_6Cl)H^+$: 313.1777, found: 313.1778.

2-Fluoro-6-chloro-9-isopropylpurine ***(4)***. Anhydrous THF (60 ml) was added under nitrogen to a flame-dried flask containing 2-fluoro-6-chloropurine (0.90 g, 5.2 mmol) and triphenylphosphine (3.0 g, 10.4 mmol). To this was added 2-propanol (800 µl, 10.4 mmol), after which the solution was cooled to −10°C. Following the dropwise addition of diethyl azodicarboxylate (850 µl, 10.4 mmol), the mixture was warmed gradually to rt. After 12 h, the reaction was quenched with water (500 µl) and the solvent removed *in vacuo*. The resulting yellow oil was purified by column chromatography (600 ml SiO_2, eluted with 100% CH_2Cl_2). The resulting solid was triturated with methanol (to remove the diethyl hydrazine-*N,N′*-dicarboxylate ester byproducts) to yield 630 mg (57 %) of **4** as a white crystalline solid. Rf 0.54 (MeOH:CH_2Cl_2 10:90); ^{1}H NMR (500 MHz, $CDCl_3$): δ 1.65 (d, 6H, J = 6.8 Hz), 4.85 (sept, 1H, 6.8 Hz), 8.15 (s, 1H); ^{13}C NMR (126 MHz, $CDCl_3$): δ 22.3, 48.4, 130.5, 143.7, 152.3, 153.1, 156.9 (J_{C-F} = 870 Hz); mass spectrum (EI$^+$) m/e 214 (M^+); anal. calc'd for $C_8H_8N_4FCl$: C, 44.77; H, 3.76; N, 26.10; Cl, 16.52. Found: C, 44.97; H, 3.76; N, 26.09; Cl 16.37.

2-Fluoro-6-(3-chloroanilino)-9-isopropylpurine ***(5)***. A mixture of **4** (3.75 g, 17.5 mmol), 3-chloroaniline (1.85 ml, 17.5 mmol) and diisopropylethylamine (3.05 ml, 17.5 mmol) were dissolved in *n*-butanol in a sealed tube. After 12 h at 140°C, the solvent was evaporated *in vacuo*, the crude product triturated with water, filtered and rinsed with CH_2Cl_2 and ether to yield 3.11 g (58%) of **5** as a white solid. Rf 0.66 (MeOH:CH_2Cl_2 5:95); ^{1}H NMR (400 MHz, $CDCl_3$) δ 1.61 (d, 6H, J = 6.8 Hz), 4.78 (sept., 1H, 6.8 Hz), 7.08 (d, 1H, J = 6.2 Hz), 7.26–7.30 (m, 1H), 7.64 (d, 1H, 8.2 Hz), 7.84 (s, 2H), 8.72 (s, 1H); ^{13}C NMR (101 MHz, $CDCl_3$) δ 22.4, 47.5, 118.9, 120.4, 123.8, 129.9, 134.4, 138.9, 139.3,150.7, 153.2(J_{C-F} = 20 Hz), 157.4(J_{C-F} = 19 Hz), 159.5; mass spectrum (EI$^+$) m/e 305 (M^+); HRMS calc'd for $(C_{14}H_{13}N_5ClF)H^+$: 305.0844, found: 305.0839; anal. calc'd for $C_{14}H_{13}N_5ClF$: C, 55.00; H 4.29; N, 22.91. Found: C, 55.35, H, 4.37, N, 23.10.

2-(1R-Isopropyl-2-hydroxyethylamino)-6-(3-chloroanilino)-9 isopropylpurine ***(60)***. Compound **6** (1.55 g, 5.1 mmol), *R*(-)2-amino-3-methyl-1-butanol (559 µl, 5.1 mmol) and diisopropylethylamine (892 µl, 5.1 mmol) were dissolved in *n*-butanol (1 ml) in a sealed tube. After heating the reaction mixture for 12 h at 140°C, the *n*-butanol was removed *in vacuo* and the crude product purified by column chromatography (400 ml SiO_2, eluted with 99:1 CH_2Cl_2:MeOH) to yield 1.2 g (57%) of **60** as a white solid. Rf 0.2 (MeOH:CH_2Cl_2 5:95); ^{1}H NMR (500 MHz, $CDCl_3$) δ 1.04 (d, 6H, 2.0, 6.8 Hz), 1.51 (d, 6H, 2.0, 6.8 Hz), 1.97–2.05 (m, 1H), 3.72–3.77 (m, 1H), 3.91–4.00 (m, 2H), 4.53 (sept., 1H, 6.8 Hz), 5.06 (d, 1H, 7.8 Hz), 6.97–7.00 (m, 1H), 7.20 (t, 3H, 8.1 Hz), 7.42 (d, 1H, 7.9 Hz), 7.55 (s, 1H), 8.00 (s, 1H), 8.03 (s, 1H); ^{13}C NMR (126 MHz, $CDCl_3$) δ 18.9, 19.4, 22.4, 30.0, 46.5, 59.6, 65.1, 114.9, 117.5, 119.6, 122.4, 129.6, 134.2, 135.1, 140.5, 150.8,

151.8, 159.7; mass spectrum (FAB+) m/e 389 (MH^+); HRMS calc'd for $(C_{19}H_{25}N_6OCl)H^+$: 389.1857, found, 389.1859; anal. calc'd for $C_{19}H_{25}N_6OCl$: C, 58.68; H, 6.48; N, 21.61; Cl, 9.12; O, 4.11. Found: C, 58.54; H, 6.61; N, 21.58; Cl, 9.10; O, 3.96.

2-Fluoro-6-(N,N'-(methyl),(3-chloroanilino)-9-isopropylpurine ***(6)***. A solution of **5** (110 mg, 0.36 mmol) in dry DMF (1.5 ml) was added dropwise to a suspension of NaH (18 mg, 0.43 mmol) in dry DMF (1 ml). This mixture was stirred for 20 min at rt, after which a solution of methyl iodide (35 µl, 0.36 mmol) in DMF (0.5 ml) was added slowly. After stirring 12 h, the DMF was removed *in vacuo* and the crude product purified by chromatography (200 ml SiO_2, eluted with 98:2 CH_2Cl_2:MeOH) to yield 115 mg of **6** (100%) as a white solid. Rf 0.61 (MeOH:CH_2Cl_2 5:95); ^1H NMR ($CDCl_3$, 400 MHz) δ 1.47 (d, 6H, 6.8 Hz), 3.73 (s, 3H), 4.68 (sept., 1H, 6.8 Hz), 7.15–7.38 (m, 5H), 7.63 (s, 1H); mass spectrum (FAB+) m/e 320 (MH^+); HRMS calc'd for $(C_{15}H_{15}N_5ClF)H^+$: 320.1080, found, 320.1080.

2-(1R-isopropyl-2-hydroxyethylamino)-6-(N,N'-(methyl),(3-chloro-anilino)-9-isopropylpurine ***(60Me)***. Procedure same as that used to prepare compound **60**. Rf 0.25 (MeOH:CH_2Cl_2 5:95); ^1H NMR (300 MHz, $CDCl_3$) δ 0.99 (d, 6H, 6.8 Hz), 1.51 (d, 6H, 6.8 Hz), 1.65 (br s, 2H), 1.94 (sept., 1H, 6.8 Hz), 3.61–3.73 (m, 2H), 3.79 (s, 3H), 4.62 (sept, 1H, 6.8 Hz), 4.83–4.85 (m, 1H), 7.19–7.36 (m, 4H), 7.49 (s, 1H); ^{13}C NMR (75 MHz, $CDCl_3$) δ 19.0, 19.4, 22.4, 22.5, 30.0, 39.8, 46.1, 59.8, 66.2, 115.6, 124.7, 126.1, 127.1, 129.7, 134.1, 134.5, 146.9, 152.5, 154.4, 159.3; mass spectrum (FAB+) m/e 403 (MH^+); HRMS calc'd for $(C_{20}H_{27}N_6OCl)H^+$: 403.2013, found, 403.2013.

2-Fluoro-6-(N-tert-butoxycarbonyl-3-chloroanilino)-9-isopropylpurine ***(7)***. Compound **5** (169 mg, 0.55 mmol), di-*tert*-butyldicarbonate (219 mg, 1.0 mmol), diisopropylethylamine (0.8 ml, 4.6 mmol) and dimethylaminopyridine (36 mg) were dissolved in THF (10 ml). After the reaction mixture was stirred at rt for 5 h, the solvent was removed *in vacuo* and the crude product was purified by column chromatography (80 ml SiO_2, eluted with ethyl acetate-hexane gradient) to yield 176 mg (79%) of 7 as a white solid. Rf 0.4 (EtOAc:hexane 1:2); ^1H NMR (500 MHz, $CDCl_3$) δ 1.47 (s, 9H), 1.63 (d, 6H, 7.0 Hz), 4.84 (m, 1H), 7.19–7.33 (m, 4H), 8.06 (S, 1H); mass spectrum (FAB+) m/e 406.1 (MH^+); HRMS calc'd for $(C_{19}H_{21}N_5O_2FCl)H^+$: 406.1446, Found 406.1437; anal. calc'd for $C_{19}H_{21}N_5O_2FCl$: C 56.23; H, 5.22; N, 17.26. Found: C, 56.48; H, 5.47; N, 16.99.

2-(1R-Isopropyl-2-hydroxyethylamino)-6-(N-tert-butoxycarbonyl-3-chloroanilino)-9-isopropylpurine ***(8)***. To a stirring solution of **7** (108 mg, 0.27 mmol) in DMSO (10 ml) was added R(-)2-amino-3-methyl-1-butanol (202 mg, 1.96 mmol) and diisopropylethylamine (1 ml, 5.7 mmol). After heating for 12 h at 80°C, the DMSO was removed *in vacuo* with heating to 70°C, and the crude product purified by chromatography (400 ml SiO_2, eluted with ethyl acetate-hexane gradient) to yield 88 mg (67%) of 8 as an oil. Rf 0.4 (EtOAc:hexane 2:1); ^1H NMR (500 MHz, $CDCl_3$) δ 0.95 (d, 3H, 7.0 Hz), 0.96 (d, 3H, 7.0 Hz), 1.47 (S, 9H), 1.57 (d, 3H, 7.0 Hz), 1.58 (d, 3H, 7.0 Hz), 1.94 (m, 1H), 3.44 (bs, 1H), 3.65 (m, 1H), 3.75–3.77 (m, 2H), 4.68 (m, 1H), 5.18 (d, 1H, 8.0 Hz), 7.21–7.31 (m, 4H), 7.77 (S, 1H); mass spectrum (FAB+) m/e 489.2 (MH^+); HRMS calc'd for $(C_{24}H_{33}N_6O_3Cl)H^+$: 489.2381, found 489.2377.

*2-(1R-isopropyl-2-dimethyl-*tert*-butylsilyloxyethylamino)-6-(N-tert-butoxycarbonyl-3-chloroanilino)-9-isopropylpurine* ***(9)***. Compound 8 (40 mg, 0.081 mmol), *tert*-butyldimethylsilyl chloride (200 mg, 1.33 mmol) and imidazole (380 mg, 5.58 mmol) were dissolved in THF (10 ml) and stirred at rt. After 24 h, a precipitate had developed which was removed by filtration. The solid byproduct was washed with THF, concentrated *in vacuo* and purified by preparative thin layer chromatography (20 × 20 cm, 0.5 mm, ethyl acetate-hexane 1:1) to give 33 mg (68%) of **9** as an oil. Rf 0.7 (EtOAc:hexane 1:1); ^1H NMR (500 MHz, $CDCl_3$) δ −0.04 (s, 3H), −0.02 (s, 3H), 0.84 (s, 9H), 0.88–0.92 (m, 6H), 1.44 (s, 9H), 1.55 (d, 3H, 7.0 Hz), 1.56 (d, 3H, 7.0 Hz), 1.97 (br, 1H), 3.59 (m, 1H), 3.70 (m, 1H), 3.82 (m, 1H), 4.69 (m, 1H), 5.06 (d, 1H, 9.5 Hz), 7.16–7.30 (m, 4H), 7.73 (s, 1H); mass spectrum (FAB+) m/e 603.3 (MH^+); HRMS calc'd for $(C_{30}H_{47}N_6O_3ClSi)H^+$: 603.3246, found 603.3247; anal. calc'd for $C_{30}H_{47}N_6O_3ClSi$: C 59.73; H, 7.85; N, 13.93. Found: C, 59.83; H, 8.04; N, 13.87.

2-(N-Benzyl-1R-isopropyl-2-hydroxyethylamino)-6-(3-chloroanilino)-9-isopropylpurine ***(301)***. To a solution of 9 (33 mg, 0.055 mmol) in DMF (7 ml) was added sequentially sodium hydride (60% dispersed in mineral oil, 94 mg, 2.4 mmol), benzyl bromide (100 µl, 0.84 mmol) and tetrabutylammonium iodide (68 mg, 0.18 mmol) at rt under nitrogen. The reaction mixture was stirred for 17 h and then diluted with CH_2Cl_2 (50 ml) and filtered through SiO_2 (100 ml). The filtrate was concentrated *in vacuo*, and hydrolysed with *p*-toluenesulfonic acid (30 mg) in a mixture of MeOH-CH_2Cl_2 (1:1, 20 ml) at rt for 24 h. After removal of the solvent, the product was purified using preparative thin layer chromatography (20 × 20 cm, 0.5 mm, ethyl acetate-hexane 2:1) to give 5 mg (19%) of 301 as an oil. Rf 0.2 (EtOAc:hexane 2:1); ^1H NMR (500 MHz, $CDCl_3$) δ 0.87 (d, 3H, 6.5 Hz), 1.08 (d, 3H, 6.5 Hz), 1.25 (s, 6H), 2.40 (m, 1H), 3.79 (m, 1H), 3.88 (m, 2H), 4.67 (m, 1H), 4.85 (br s, 2H), 6.99 (br, 1H), 7.12–7.96 (m, 10H); mass spectrum (FAB+) m/e 479.2 (MH^+); HRMS calc'd for $(C_{26}H_{31}N_6OCl)H^+$: 479.2326, found 479.2321.

Supplementary material

General synthetic methods and spectroscopic data for all compounds included in the main text, as well as details of solid-phase synthesis of representative library members and all biological assays (kinase assays, cell culture, cell viability assays, cell-cycle and apoptosis assays, flow cytometry and cell-cycle analysis and immunocytochemistry) are published with the online version of this paper.

Acknowledgements

We thank Ulrich Wendt for producing the stereo images and the NCI for cellular assays. We gratefully acknowledge the financial support of CaP CURE. Y.T.C. wishes to acknowledge the financial support of Korea Research Foundation and N.S.G. is supported by a NSF predoctoral fellowship. L.M. was supported by grants from the Association pour la Recherche sur le Cancer (ARC 9314) and the Conseil Regional de Bretagne.

References

1. Hodges, P.E. (Ed). *Yeast Proteome Handbook* (1998, 5th ed.), Proteome, Inc., Beverly, USA.
2. Vesely, J., *et al.*, & Meijer, L. (1994). Inhibition of cyclin-dependent kinases by purine analogues. *Eur. J. Biochem.* **224**, 771-786.
3. Meijer, L. *et al.*, & Moulinoux, J.-P. (1997). Biochemical and cellular effects of roscovitine, a potent and selective inhibitor of the cyclin-dependent kinases cdc2, cdk2 and cdk5. *Eur. J. Biochem.* **243**, 527-536.
4. Schulze-Gahmen, U. *et al.*, & Kim, S.-H. (1995). Multiple modes of ligand recognition – crystal structure of cyclin dependent protein kinase 2 in complexes with ATP and two inhibitors, olomoucine and isopentenyladenine. *Proteins* **22**, 378-391.
5. Nigg, E.A. (1995). Cyclin-dependent protein kinases – key regulators of the eukaryotic cell cycle. *BioEssays* **17**, 471-480.
6. Norman, T.C., Gray, N.S., Koh, J.T. & Schultz, P.G. (1996). A structure-based library approach to kinase inhibitors. *J. Am. Chem. Soc.* **118**, 7430-7431.
7. Gray, N.S., Kwon, S. & Schultz, P.G. (1997). Combinatorial synthesis of 2,9-substituted purines. *Tetrahedron Lett.* **38**, 1161-1164.
8. Nugiel, D.A., Cornelius, L.A.M. & Corbett, J.W. (1997). Facile preparation of 2,6-disubstituted purines using solid-phase chemistry. *J. Org. Chem.* **62**, 201-203.
9. Legraverend, M., Ludwig, O., Bisagni, E., Leclerc, S. & Meijer, L. (1998). Synthesis of C2 alkynylated purines, a new family of potent inhibitors of cyclin-dependent kinases. *Bioorg. Med. Chem. Lett.* **8**, 793-798.
10. Schow, S.R., *et al.*, & Lum, R.T. (1997). Synthesis and activity of 2,6,9-trisubsituted purines. *Bioorg. Med. Chem. Lett.* **7**, 2697-2702.
11. Fiorini, M.T. & Abell, C. (1998). Solution-phase synthesis of 2,6,9-trisubstituted purines. *Tetrahedron Lett.* **39**, 1827-1830.
12. de Azevedo, Jr., W.F., Mueller-Diechmann, H.-J., Schulze-Gahmen, U., Worland, P.J., Sausville, E. & Kim, S.-H. (1996). Structural basis for specificity and potency of a flavonoid inhibitor of human CDK2, a cell cycle kinase. *Proc. Natl Acad. Sci. USA* **93**, 2735-2740.

13. Lawrie, A.M., Noble, M.E.M., Tunnah, P., Brown, N.R., Johnson, L.N. & Endicott, J.A. (1997). Protein kinase inhibition by staurosporine revealed in details of the molecular interaction with CDK2. *Nat. Struct. Biol.* **4**, 796-801.
14. Toyota, A., Katagiri, N. & Kaneko, C. (1993). The alkylation of 2-amino-6-chloropurine with alcohols by Mitsunobu reaction for a synthesis of carbocyclic guanosine analogs. *Heterocycle* **36**, 1625-1630.
15. Legraverend, M., *et al.*, & Fovaudon, V. (1999). *Bioorg. Med. Chem.*, in press.
16. Gray, N.S., *et al.*, & Schultz, P.G. (1998). Exploiting chemical libraries, structure and genomics in the search for kinase inhibitors. *Science* **281**, 533-538.
17. Hansen, M.B., Nielsen, S.E. & Berg, K.J. (1989). Re-examination and further development of a precise and rapid dye method for measuring cell growth/cell kill. *Immunol. Methods* **119**, 203-210.
18. Guadagno, T.M. & Newport, J.W. (1996). CDK2 kinase is required for entry into mitosis as a positive regulator of cdc2-cyclin B kinase activity. *Cell* **84**, 73-82.
19. Hinchliffe, E.H., Cassels, G.O., Rieder, C.L. & Sluder, G. (1998). The coordination of centrosome reproduction with nuclear events of the cell cycle in the sea urchin zygote. *J. Cell Biol.* **140**, 1417-1426.
20. Schutte, B., Nieland, L., van Engeland, M., Henfling, M.E.R., Meijer, L. & Ramaekers, F.C.S. (1997). The effect of the cyclin-dependent kinase inhibitor olomoucine on cell cycle kinetics. *Exp. Cell Res.* **236**, 4-15.
21. Planchais, S. *et al.*, & Bergounioux, C. (1997). Roscovitine, a novel cyclin-dependent kinase inhibitor, characterizes restriction point and G2/M transition in tobacco BY-2 cell suspension. *Plant J.* **12**, 191-202.

Because *Chemistry & Biology* operates a 'Continuous Publication System' for Research Papers, this paper has been published via the internet before being printed. The paper can be accessed from http://biomednet.com/cbiology/cmb – for further information, see the explanation on the contents pages.